Geometry Textures

Rodrigo de Toledo
Tecgraf – PUC-Rio
Rio de Janeiro - RJ, Brasil
rtoledo@tecgraf.puc-rio.br

Bin Wang
School of Software
Tsinghua University, China
binwang@gmail.com

Bruno Lévy
INRIA – ALICE
Villers-lès-Nancy, France
Bruno.Levy@inria.fr

Abstract

In highly tessellated models, triangles are very small compared to the entire object, representing at the same time its macro- and mesostructures. The main idea in this work is to use a visualization algorithm that is adequate to mesostructure but applied to the whole object. Tessellated models are converted into geometry textures*, a geometric representation for surfaces based on height maps. In rendering time, the fine-scale details are reconstructed with LOD speed-up while preserving original quality.*

1 Introduction

The goal of *geometry textures* is to interactively display finely tessellated geometric models. Nowadays, models with millions of triangles still cannot be directly rendered by graphics cards without using elaborate acceleration methods. The large number of triangles overloads the vertex pipeline of the GPU. In our work, the geometry is no longer represented by polygons and the main rendering effort is on the pixel pipeline, alleviating the vertex one, thus allowing a significant increase in performance. Transferring the workload to the pixel pipeline brings the benefit of a natural LOD, since rendering time is proportional to the number of rendered pixels. Therefore, when a complex object is far away from the viewer, less computation must be done.

The main idea in our technique is to reconstruct the fine-scale geometric details over a simple proxy of the original model. Fine-scale geometric details are known in the literature as *mesostructure*. Mesostructures are commonly simulated as a pattern in visualization systems. Its simplest representation is the *color map*, which is a 2D image applied over a virtual object. Other possible mesostructure representations are bump maps, height maps and volumes. More complex representations store the whole shading function over surfaces. In rendering time, the mesostructure is repetitively applied all over a simple mesh to obtain the details.

Differently from standard mesostructure rendering, we want to reconstruct the complete object. In our case, the mesostructure changes along the object surface, and memory becomes an issue. For this reason we are interested in height maps, which are a compact way to represent surfaces. Although usually applied to terrains, height maps are used to represent the mesostructure over macro surfaces. The map domain is no longer a plane, but it is adjusted to the geometry curvature (as in texture mapping). Displacement mapping [3], VDM [10] and Relief Texture Mapping [5, 6] are some examples of height-map mesostructure representations.

In our technique, the input is a set of height maps generated from the original model to represent the real geometry information. We directly use the maps during rendering, executing a ray-casting algorithm implemented in GPU. In our approach, the geometry is passed to the GPU as a texture (the geometry texture), which is used by the fragment shader. There is no need to reconstruct any triangle and almost all the effort is done per fragment. Our fragment shader renders the geometry with the correct z-buffer output information. This means that the *geometry textures* are compatible with standard GPU primitives (and also compatible with themselves). Geometry details are reconstructed with the correct shading, self-occlusion and silhouette.

2 Related Work

The first technique that used height map to represent mesostructure was displacement mapping [3]. It subdivides the macro geometry into a large number of small polygons whose vertices are displaced in the normal direction according to the associated displacement map. Its drawback is the excessive number of generated polygons.

To avoid extra polygons, the VDM method (View-dependent Displacement Mapping [10]) adopts the idea of previously sampling mesostructure appearance under various lighting and view directions. In preprocessing, a height map is taken as input and synthesizes a set of VDM images for different view directions and different curvatures, recording the VDM data as a 5D function. Although result-

ing in good quality, this method transforms a 16KB map into a 64MB volume of data, which prevents its application for our purpose, since we use hundreds of maps.

RTM (*Relief Texture Mapping* [5]) is the first work on object visualization based on multiple height maps. RTM starts by capturing the depth of an object from six orthogonal points of view. In rendering time, a warping-based technique is applied on the faces of the bounding box to reconstruct the original model. Later, Policarpo et al. [6] extended RTM to interactive mesostructure visualization. Their method is the most similar to ours. However, they devote their attention to mesostructures, and not to complex and highly-tessellated surfaces.

Badoud and Décoret [1] also use multiple height maps to represent and render complex objects. They store the height maps of the six orthogonal points of view using an adapted perspective frustum, which increases the detail information about features that are almost perpendicular to the view point. During rendering, they use a clipped frustum to reduce the number of discarded fragments.

Porquet et al. [7] have developed a technique to render complex surfaces by using a rough geometric approximation on which colors and normals are applied according to previously captured information, including height maps. In preprocessing, they capture the maps from several points of view. In rendering time, the three closest views to the camera projection are used by the fragment shader. Based on the height maps, the fragment shader reconstructs the equivalent information of the three points of view to finally find which one is the nearest sample to the current fragment, defining the color and the normal to be used. The main disadvantage of this method is the lack of silhouette details.

The *multi-chart geometry images* method [9] is similar to our geometry textures method, although it does not use height maps. It extends *Geometry images* [4] by splitting a model into multi charts before parameterizing each one onto a square. It is especially different from our method during rendering. To render the geometry images, it is necessary to reconstruct many triangles from the images, overcharging the vertex pipeline, which is exactly what we want to avoid.

3 Geometry Texture Rendering

3.1 Height-map GPU ray casting

A height map (a.k.a. height field, relief map or depth texture) is a 2D regular table where a height is specified for each entry. One way of representing a height map is a grayscale image with brightness representing height (see Figure 2(a)). Terrains are an example of a surface well suited to be represented by height maps.

A height map can be represented by the function:

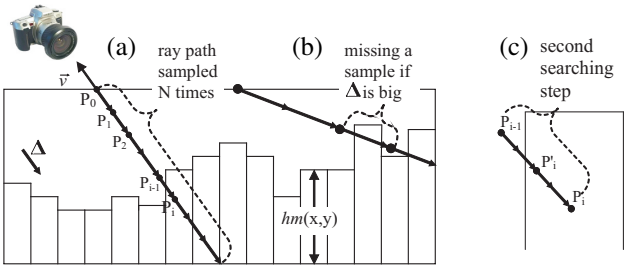

Figure 1. Height-map cut view. (a) Searching for the intersection; (b) large Δ could result in missing information; (c) a second searching step is done to refine the intersection point.

$$hm(x, y) : [0, 1]^2 \rightarrow [0, 1].$$

We can define a Boolean function $z(P)$, for $(P.x, P.y, P.z) \in [0, 1]^3$, as:

$$z(P) \Leftarrow (\ P.z \leq hm(P.x, P.y)\ )\ ?\ \text{true} : \text{false},$$

In our implementation, we use the faces of a parallelepiped to generate the fragments that will ray cast the height map. The coordinates of its vertices are between 0 and 1 (as in a canonical cube), defining the local coordinate space. The height map data is passed to the GPU through a grayscale texture. The x and y axes of the parallelepiped are exactly coincident with the u and v coordinates of the texture, while z coincides with the height direction.

In GPU, the vertex shader sends to the fragment shader the viewing direction already in local space. This way, each fragment knows the path of the ray inside the canonical cube, and can easily compute its exit point. The fragment shaders main task is to answer the two ray-casting questions: is there an intersection between the ray and the height map? Where is the closest hit point?

As explained in [6], one strategy is to uniformly sample this ray path in N points P_i (see Figure 1(a)) and use function $z(P)$ to find the ray-surface intersection. This could be implemented by a conditional loop varying P_i, from the entering to the exit point, and stopping when $z(P_i)$ is false. In each step P_i is translated by Δ, which is the ray path divided by N.

```
RayCasting()
{
   P: Point3D
   P ⇐ ray_origin
   Δ ⇐ (exit_point - ray_origin) / N
   while ( P ≠ exit_point  and  !z(P))
     P ⇐ P + Δ
}
```

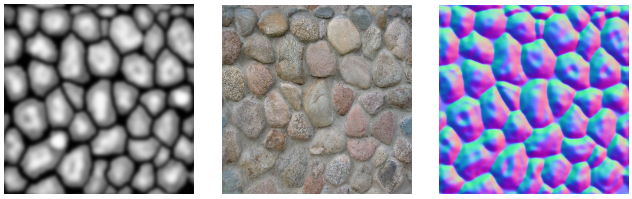

(a) (b) (c)

Figure 2. From left to right: the height map, the color map, and the normal map.

When a ray does not intersect any height sample, the fragment should be discarded without any contribution to the frame buffer or to the z-buffer. For fragments not discarded, the actual color can be retrieved from a color texture (see Figure 2(b)), and the normal can be either computed directly from the height map or given as a third texture (see Figure 2(c)) to be used for shading. The coordinates used in the texture lookup are $(P.x, P.y)$ right after the iterations. Finally, the depth is computed to register the correct z-value for the z-buffer.

The value of N is a trade off between quality and speed. Some ray-surface intersections may be missed if a large Δ is used (Δ is inversely proportional to N, see Figure 1(b)).

We propose the following improvements for the height-map GPU visualization:

Two-step searching. Even if Δ is short enough not to miss a sample, the point where the ray touches the object is not exactly computed. We propose a second searching step between points P_{i-1} and P_i (see Figure 1(c)). This second step is a binary search that divides the searching domain by two in each step. Therefore, with M steps in the binary search we multiply the precision by a 2^M factor. Notice that this second searching procedure is done in the same fragment code, it is not a multi-pass algorithm.

Balancing between steps. Binary search is much more efficient than linear search. However, it cannot be exclusively executed because, along the ray path, there could be several intersections. In other words, the $z(P)$ function may change different times along the parametric ray for each fragment. On the other hand, when the ray is totally perpendicular to the height map (in a perfect top view), $z(P)$ will change sign at most once. In this case, the binary search can perfectly and efficiently compute the intersection without the previous linear search. Based on this observation, we have implemented a balance between the linear and the binary steps according to the viewing slant. When in a vertical view, we reduce the linear search iterations while increasing the binary search iterations ($N\downarrow$, $M\uparrow$). For an almost horizontal viewing direction we do the opposite, prioritizing the linear search ($N\uparrow$, $M\downarrow$). This way, we achieve up to two times faster rendering for some cases (see Figure 3).

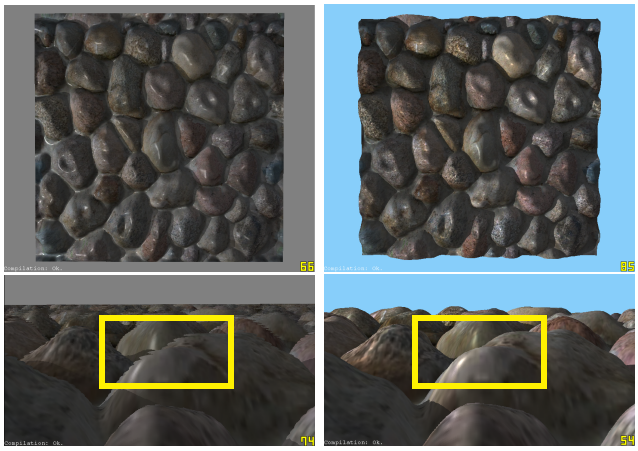

Figure 3. Comparing not-balanced [6] and balanced searches (right column). We obtain better performance when seen from above and better quality when seen in a profile view.

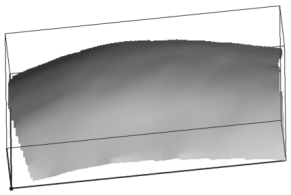

Figure 4. Geometry texture sample. A height map defined inside a hexahedron's domain.

Non-rectangular height map domain. A height sample with value equal to 0 can be considered either as the surface base or as a representation of empty space. We have chosen the last case, since representing empty space is essential for geometry textures. Figure 6(d) has an example.

3.2 Geometry Textures

The problem approached in our work is different from standard mesostructure rendering. We are interested in reconstructing the details of an entire object, which is a non-repetitive pattern, since it changes over the model domain. In our case, the input is a set of height maps converted from the original model to represent the complete geometrical information.

Geometry texture is a geometric representation for surfaces. Its domain is a parallel hexahedron and in its interior a height-map represents the surface (see Figure 4). The domain is not restricted to a perfect rectangle, so empty samples are expected in each geometry texture. The construction of geometry texture patches from a complex model has

no global folding restriction and the patches are well fitted around the surface contour. In rendering time, geometry textures use our ray-casting algorithm implemented in a fragment shader. As a result, the geometry is correctly reconstructed and rendered.

4 Conversion

The input for our conversion procedure is a polygon mesh and the output is a set of geometry textures. Figure 5 shows the complete algorithm for converting triangle meshes into geometry textures.

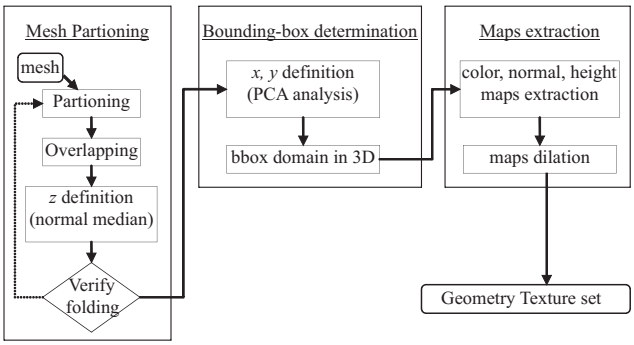

Figure 5. Complete procedure for converting polygon meshes into a set of geometry textures. Note that the *verify folding* step sends a chart back to the *partitioning* step in case of a overhanging situation.

Among the three conversion steps, *mesh partitioning* is the most difficult and critical for the success of the algorithm. Some conditions are expected when partitioning the input model mesh into charts:

- The chart must not contain a folding situation in its $\vec{z}$.
- The chart domain should be as square as possible to reduce empty spaces.
- For visualization purposes, neighboring charts must share their boundary, resulting in some overlapping between them. Right after partitioning we add an extra triangle ring around each chart (see Figure 6b).

Bounding-box determination includes finding a good orthonormal coordinate system and domain for each one of the charts. Direction $\vec{z}$ is taken as the median normal of all triangles in one chart, with this we minimize the occurence of self-folding partitions. Then, $\vec{x}$ and $\vec{y}$ must be chosen based on the minimization of empty spaces in the domain. We have used the 2D-PCA (Principal Component Analysis)

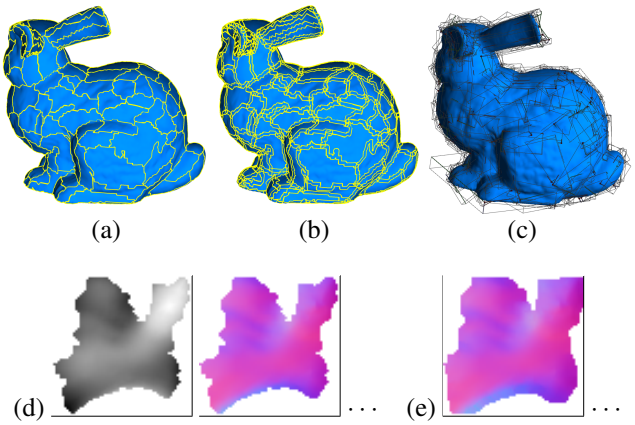

Figure 6. (a) Mesh partitioning using VSA. (b) Overlapping step, each chart is increased by one ring of triangles. (c) Bounding-box determination. (d) Map extraction (height and normal). (e) Map dilation (two-pixel dilation).

algorithm to determine directions $\vec{x}$ and $\vec{y}$ projected on the plane defined by $\vec{z}$. Finally, we project the coordinates of all triangles to obtain the exact domain in each direction. $(\vec{x}, \vec{y}, \vec{z})$ forms the local coordinate system of the chart.

In the *map extraction* phase, there are three maps we want to obtain: height, color and normal maps. We have developed a GPU solution to extract the three maps from one chart. Based on the local coordinate system of each chart, we render its triangles in an orthogonal view projection perpendicularly to direction $\vec{z}$, filling out the viewport with a user-defined resolution (for example, 256×256). We repeat the procedure three times capturing the image buffer:

- To obtain the *color map* we render the colors without illumination.
- To generate the *normal map* we assign (x, y, z) global coordinates of normal $\vec{n}_i$ of each vertex v_i to (r, g, b). During rasterization, within each triangle, the normals are interpolated and then normalized again.
- To obtain the *height map* we start by finding in CPU the maximum and minimum coordinates (h_{max} and h_{min}) in direction $\vec{z}$. We assign a value $h_i \in [0, 1]$, computed as $h_i = \frac{v_i.z - h_{min}}{h_{max} - h_{min}}$, to each vertex v_i. This value is interpolated inside the triangles and outputted as luminance.

Note that for space-reduction purposes, the image buffer is captured and stored using 8-bit precision.

The rendering algorithm loads the maps as textures. However, before that, we apply a texel-dilation procedure to prevent sampling problems when using mip-mapping. Our

dilation algorithm fills empty texels around the map domain with interpolated values. This procedure is done for normal and color maps. See Figure 6.

In the following subsections we discuss two different strategies we have implemented for mesh partitioning: PGP (Periodical Global Parameterization [8]) and VSA (Variational Shape Approximation [2]).

4.1 Partitioning with PGP

Periodic Global Parameterization is a globally smooth parameterization method for surfaces. PGP can be applied to meshes with arbitrary topology, which is a restriction in other parameterization methods [8]. Moreover, we can extract a quadrilateral chart layout from this parameterization, which is based on two orthogonal piecewise linear vector fields defined over the input mesh. This orthogonality is especially interesting to guide our partitioning procedure in order to reduce empty spaces in the domain. These vector fields are obtained by computing the principal curvature directions, resulting in a parameterization that follows the natural shape of the surface (left picture on Figure 7).

PGP avoids excessive empty spaces. However, often charts obtained with PGP partitioning present some folding problems. For this reason we have decided to investigate VSA as an alternative partitioning method.

4.2 Partitioning with VSA

Variational Shape Approximation is a clustering algorithm for polygonal meshes that can be used for geometry simplification [2]. Our partitioning algorithm based on VSA uses each cluster as an initial chart, which is further increased to overlap neighboring domains (see Figure 6).

The main advantage of using VSA compared to PGP is that it reduces the number of folding cases. VSA uses $\mathcal{L}^{1,2}$ metric, which is based on the $\mathcal{L}^2$ measure of the normal field. This means that it takes into account the normal direction of the vertices to cluster them. A folding situation occurs only if vertices in a chart have a sharp difference in their normal direction (over 90 degrees). With VSA, each chart only contains vertices with similar normal directions.

In the next section we describe some experiments to compare the PGP and the VSA methods.

4.3 Comparing PGP and VSA

In our tests we have partitioned with both PGP and VSA two different models: bunny and buffle (Figures 6 and 7).

Our first test compares how good PGP and VSA are at avoiding empty spaces. We have counted for each chart the number of used and empty texels. This was done in the four test cases (PGP bunny, VSA bunny, PGP buffle and VSA buffle). For simplicity, the charts were extracted without overlapping and the maps without dilation. The maximum map size was 128×128. A map could be smaller than that (adapted to the chart size), as long as each dimension remained a power of two (respecting OpenGLs restriction). Table 1 shows the results, indicating that PGP is better at avoiding empty spaces.

Model	Method	Total texels	Empty texels	%
Bunny	PGP	1008128	240357	23.84%
Bunny	VSA	461312	179194	38.84%
Buffle	PGP	2498048	563652	22.56%
Buffle	VSA	979456	453069	46.25%

Table 1. Considering empty spaces, PGP is the best partitioning method.

In our second test we have counted how many charts have folding problems, again in the four test scenarios. A way to check if a chart has a folding situation is to verify if there is any *inverted triangle* when rasterizing all triangles in local direction $\vec{z}$. Given that the triangles in the mesh respect a counterclockwise rotation, if at least one of them is rasterized clockwise then the mesh folds itself in direction $\vec{z}$. Figure 7 shows a partitioned buffle model with inverted triangles marked in green. In Table 2 we present the number of folding charts and the total number of inverted triangles found. Clearly, VSA is more appropriate to avoid folding problems.

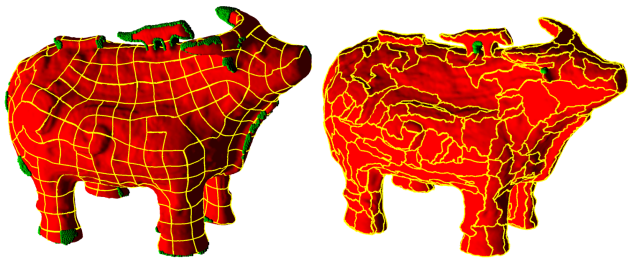

Figure 7. Buffle partitioning with PGP and with VSA. Triangles with folding problem have their vertices marked in green.

In conclusion, both methods have their own advantages. While PGP is better for reducing empty spaces, VSA is much more efficient in avoiding self-folding charts. We consider that the folding problem is the most important issue. Self-folding charts cannot be represented by our geometry texture, which is a strong restriction. On the other hand, empty-space reduction is merely an optimization.

Based on these facts, we have chosen VSA as our partitioning method (see the total conversion time in Table 3).

Model	Method	Initial triangles	Initial charts	Inverted triangles	Folding charts
Bunny	PGP	69,451	224	817	45
Bunny	VSA	69,451	222	3	3
Buffle	PGP	117,468	403	2819	62
Buffle	VSA	117,468	397	34	6

Table 2. VSA significantly reduces the number of folding charts (identified by inverted triangles).

The results presented in the next section have been achieved using VSA.

Model	VSA	Bbox	Maps	Total	Memory
Bunny	168.9s	6.5s	8.8s	3min 4.2s	1.76MB
Buffle	184.4s	20.5s	14.6s	3min 39.5s	3.73MB

Table 3. Conversion times for bunny (222 charts) and buffle (220 charts) using VSA (128×128 map size). Most of the effort is in the partitioning step. The last column shows the memory size of generated maps.

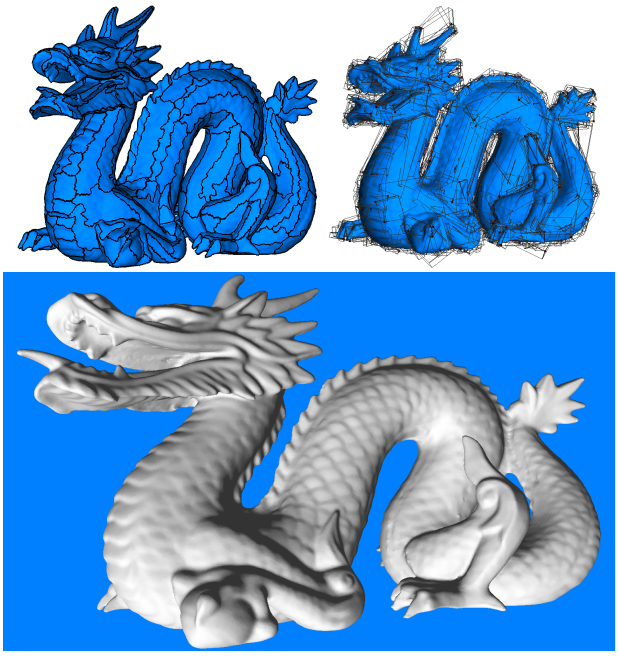

Figure 8. *Top:* **Model partitioning and geometry-texture bounding boxes.** *Bottom:* **The dragon rendered with 453 geometry textures with maximum resolution** 256×256**.**

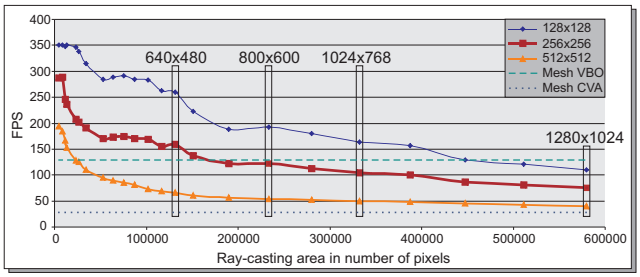

Figure 9. We have compared three different geometry texture resolutions (128^2, 256^2, 512^2) and the original mesh rendered with VBO (Vertex Buffer Object) and CVA (Compiled Vertex Array) of the dragon model.

5 Results

Once we have obtained a set of geometry textures, we can render them using the GPU height-map ray-casting algorithm. In the following sections we discuss performance, rendering quality and memory use.

We have used the dragon model with 871,414 triangles for tests (see Figure 8). We have generated three sets of 453 geometry textures, varying their maximum resolution (128^2, 256^2 and 512^2). The tests were done with a GeForce 8800 GTX graphics card.

5.1 Performance

Since geometry textures have their performance bottlenecked per pixel, we have varied the zoom level in our tests. We have plotted the results in Figure 9.

To compare performance between geometry textures and common triangle-mesh visualization, we have measured the rendering speed of the original dragon model in two special situations: with *Compiled Vertex Array* (CVA) and with *Vertex Buffer Object* (VBO). Both methods are advanced features in OpenGL and without them the speed would be less than 1 FPS for such model size. For the dragon model with 871K triangles, we have obtained 27 FPS with CVA and 135 FPS with VBO (plotted as dashed lines in Figure 9).

The horizontal axis in Figure 9 represents the number of pixels of the dragon's *ray-casting area*, which is formed by the rasterization of the geometry-textures bounding-box faces (without recounting overlapping fragments). The higher the number of pixels, the larger the model is on the screen. For a practical idea, we have highlighted some window sizes (640×480, 800×600, 1024×768, 1280×1024) which the model would fit.

The ray-casting algorithm is the same independently of

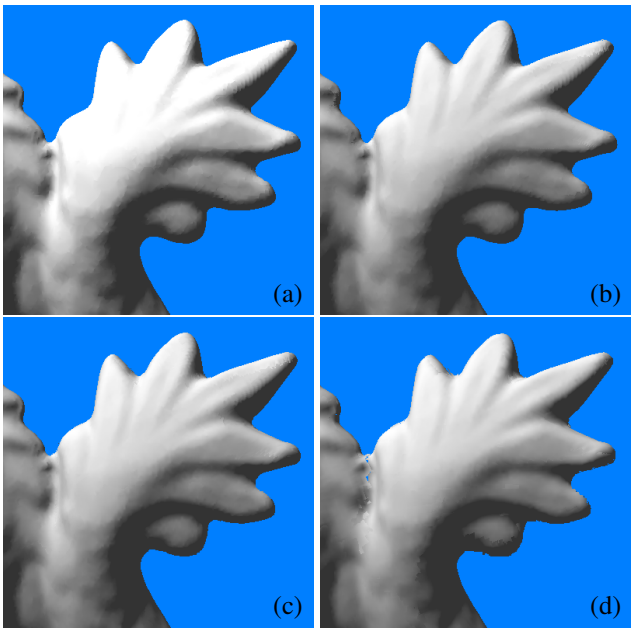

Figure 10. (a) Original dragon model with 800K triangles. Dragon rendering with geometry textures in different resolutions: (b) 512×512**; (c)** 256×256**; and (d)** 128×128**.**

resolution. However, we have verified that the lowest maximum resolution (128^2) was the fastest one. This is a result of less graphics card memory in use (4.21MB), optimizing caching and fetching. As we will see, for quality purposes, 256^2 would be a good choice for maximum resolution for the dragon's 453 geometry textures used in test. Its performance is better than the original mesh rendered with VBO for resolutions smaller than 800×600.

5.2 Quality

We have compared image quality by rendering the three sets of geometry textures for the dragon model and its original mesh. Most visual differences among the four situations appear in the silhouette. For this reason, in Figure 10 we focus on the dragon tail. Geometry textures with 256^2 and 512^2 are very close to the original mesh rendering. Based on this observation (which is the same for the whole model), there is no reason in using resolution 512^2 in this case, which would multiply by four the memory size compared to 256^2. However, geometry textures with resolution 128^2 produce an imprecision visible all over the model.

Seamless Rendering

Since we are rendering a model as a composition of patches, an important issue is to assure the continuity of the reconstruction. A perfect junction is possible due to two details in our technique, as has been previously described. The first one is in conversion time: for each patch an extra ring of triangles from the neighboring patches (in the dragon example, we have used four extra rings) is used to generate the geometry textures. The overlap area is necessary to avoid cracks. The second detail refers to the rendering algorithm, and it is based on the fact that the correct z-buffer information is generated. As shown in Figure 11, continuity is also guaranteed by the correct computation of the final shading over the overlapping parts, based on the normal maps. Per-fragment depth information is also important to maintain compatibility with any other object rendered in the scene.

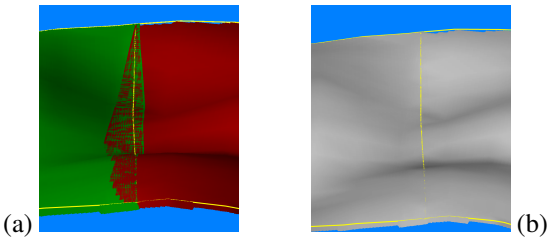

Figure 11. Even if continuous fragments are not rendered by the same geometry texture (a), the final image has no seams (b). There is a *z-fighting* **in the overlapping part, but they are fighting for the same final color.**

5.3 Memory

Memory usage is quadratically proportional to the maximum geometry-texture resolution size. In the dragon example we have obtained: $128^2 \rightarrow$4.12MB; $256^2 \rightarrow$20.0MB; and $512^2 \rightarrow$80.6MB. The dragon's original mesh uses 13.3MB. We have observed in the discussion about quality that the recommended resolution in our tests was 256^2, which has a size compatible to the original model. If memory becomes an issue, then 128^2 could be used with the drawback of some precision loss.

6 Conclusion and Future Work

We have proposed a new representation for highly-tessellated models using a set of geometry textures, which are rendered using a GPU implementation of height-map ray casting. Our results have shown that this new representation is suitable for natural models. The final rendered images have similar quality compared to traditional polygonal rasterization methods.

The following items are some of the positive aspects of our technique:

- The rendering speed naturally follows a LOD behavior. This means that when the model is small on the screen (i.e., far from the camera), rendering is faster. This is a result of relieving the vertex-stage burden, transferring computation bottleneck to pixel stage.

- Depending on the chosen resolution, our representation requires less memory than polygonal representation, without losing significant geometry information.

- Our technique is compatible with polygon rasterization, thus geometry-texture objects can be inserted in any virtual scene composed by polygonal objects.

Our potential drawbacks are:

- Recent graphics cards that implement VBO extension have very high performance for polygonal rendering. As a consequence, when compared to VBO performance, our technique is faster only if the model is not so big on the screen. However, if the scene contains multiple models, polygonal rendering would proportionally lose performance, while our solution would keep a stable frame rate.

- Another adverse point is the sophisticated conversion algorithm. Our procedure is composed by multiple passes, including the partitioning step, which is considerably elaborate. This may be improved by using multilayer height map (see next section).

We suggest the following ideas for future work:

Image operations on geometry textures. Once we have a new geometry representation based on images (height maps), image operations can be applied on these maps to obtain new results. For example, one could use a low-band filter to smooth the geometry (or a high-band filter to highlight small geometric features). Image operations to transform geometry is a promising application.

Multilayer height-map. The idea is to have only one "geometry texture" to represent the entire model, but with multiple height maps. A unique bounding-box could be used, setting a global height direction ($\vec{z}$). Multiple height-maps can be obtained from the polygonal geometry based on $\vec{z}$. In rendering time, a multilayer height-map is rendered also using per-fragment ray casting, considering the layers as forming a CSG (Constructive Solid Geometry) model. Compared to geometry textures, multilayer height-map may have some advantage in reducing implementation complexity. In preprocessing, it would skip partitioning and overlapping steps.

References

[1] L. Baboud and X. Dcoret. Rendering geometry with relief textures. In *GI '06: Proceedings of the 2006 conference on Graphics interface*, pages 195–201, Toronto, Ont., Canada, Canada, 2006. Canadian Information Processing Society.

[2] D. Cohen-Steiner, P. Alliez, and M. Desbrun. Variational shape approximation. *ACM Transactions on Graphics. Special issue for SIGGRAPH conference*, pages 905–914, 2004.

[3] R. L. Cook. Shade trees. In *Proceedings of the 11th annual conference on Computer graphics and interactive techniques*, pages 223–231. ACM Press, 1984.

[4] X. Gu, S. J. Gortler, and H. Hoppe. Geometry images. In *SIGGRAPH '02: Proceedings of the 29th annual conference on Computer graphics and interactive techniques*, pages 355–361, New York, NY, USA, 2002. ACM Press.

[5] M. M. Oliveira, G. Bishop, and D. McAllister. Relief texture mapping. In *Proceedings of ACM SIGGRAPH 2000*, Computer Graphics Proceedings, Annual Conference Series, pages 359–368, July 2000.

[6] F. Policarpo, M. M. Oliveira, and J. L. D. Comba. Real-time relief mapping on arbitrary polygonal surfaces. In *SI3D '05: Proceedings of the 2005 symposium on Interactive 3D graphics and games*, pages 155–162, New York, NY, USA, 2005. ACM Press.

[7] D. Porquet, J.-M. Dischler, and D. Ghazanfarpour. Real-time high-quality view-dependent texture mapping using per-pixel visibility. In *GRAPHITE '05: Proceedings of the 3rd international conference on Computer graphics and interactive techniques in Australasia and South East Asia*, pages 213–220, New York, NY, USA, 2005. ACM Press.

[8] N. Ray, W. C. Li, B. Lévy, A. Sheffer, and P. Alliez. Periodic global parameterization. *ACM Trans. Graph.*, 25(4):1460–1485, 2006.

[9] P. V. Sander, Z. J. Wood, S. J. Gortler, J. Snyder, and H. Hoppe. Multi-chart geometry images. In *SGP '03: Proceedings of the 2003 Eurographics/ACM SIGGRAPH symposium on Geometry processing*, pages 146–155, Aire-la-Ville, Switzerland, 2003. Eurographics Association.

[10] L. Wang, X. Wang, X. Tong, S. Lin, S. Hu, B. Guo, and H.-Y. Shum. View-dependent displacement mapping. *ACM Transactions on Graphics*, 22(3):334–339, July 2003.